



Ultra-large core birefringent Yb-doped tapered double clad fiber for high power amplifiers

ANDREY FEDOTOV,^{1,*} TEPPONORONEN,² REGINA GUMENYUK,¹ VASILIIY USTIMCHIK,^{3,4} YURI CHAMOROVSKII,⁴ KONSTANTIN GOLANT,⁴ MAXIM ODNOLYUDOV,⁵ JOONA RISSANEN,¹ TAPIO NIEMI,¹ AND VALERY FILIPPOV⁵

¹Tampere University of Technology, Korkeakoulunkatu 3, 33101 Tampere, Finland

²Ampliconyx Ltd, Lautakatonkatu 18, 33580 Tampere, Finland

³Kotel'nikov Institute of Radioengineering and Electronics of RAS, 11-7 Mokhovayast, Moscow, 125009, Russia

⁴Moscow Institute of Physics and Technology, 9 Institutskiy per., Dolgoprudny, Moscow Region, 141701, Russia

⁵Peter the Great St. Petersburg State Polytechnical University, Polytechnicheskaya str.29, 195251 St. Petersburg, Russia

*andrei.fedotov@tut.fi

Abstract: We present a birefringent Yb-doped tapered double-clad fiber with a record core diameter of 96 μm . An impressive gain of over 38 dB was demonstrated for linearly polarized CW and pulsed sources at a wavelength of 1040 nm. For the CW regime the output power was 70 W. For a mode-locked fiber laser a pulse energy of 28 μJ with 292 kW peak power was reached at an average output power of 28 W for a 1 MHz repetition rate. The tapered double-clad fiber has a high value of polarization extinction ratio at 30 dB and is capable of delivering the linearly polarized diffraction-limited beam ($M^2 = 1.09$).

© 2018 Optical Society of America under the terms of the OSA Open Access Publishing Agreement

OCIS codes: (060.2320) Fiber optics amplifiers and oscillators; (060.3510) Lasers, fiber; (060.2420) Fibers, polarization-maintaining.

References and links

1. J. P. Koplow, D. A. V. Kliner, and L. Goldberg, "Single-mode operation of a coiled multimode fiber amplifier," *Opt. Lett.* **25**(7), 442–444 (2000).
2. J. Limpert, N. Deguil-Robin, I. Manek-Hönninger, F. Salin, F. Röser, A. Liem, T. Schreiber, S. Nolte, H. Zellmer, A. Tünnermann, J. Broeng, A. Petersson, and C. Jakobsen, "High-power rod-type photonic crystal fiber laser," *Opt. Express* **13**(4), 1055–1058 (2005).
3. P. Wang, L. J. Cooper, J. K. Sahu, and W. A. Clarkson, "Efficient single-mode operation of a cladding-pumped ytterbium-doped helical-core fiber laser," *Opt. Lett.* **31**(2), 226–228 (2006).
4. S. Lefrancois, T. S. Sosnowski, C.-H. Liu, A. Galvanauskas, and F. W. Wise, "Energy scaling of mode-locked fiber lasers with chirally-coupled core fiber," *Opt. Express* **19**(4), 3464–3470 (2011).
5. V. Filippov, Y. Chamorovskii, J. Kerttula, K. Golant, M. Pessa, and O. G. Okhotnikov, "Double clad tapered fiber for high power applications," *Opt. Express* **16**(3), 1929–1944 (2008).
6. <http://www.nktp Photonics.com/product/aerogain-rod-high-power-ytterbium-rod-fiber-gain-modules/>
7. T. Eidam, J. Rothhardt, F. Stutzki, F. Jansen, S. Hädrich, H. Carstens, C. Jauregui, J. Limpert, and A. Tünnermann, "Fiber chirped-pulse amplification system emitting 3.8 GW peak power," *Opt. Express* **19**(1), 255–260 (2011).
8. V. Filippov, Yu. Chamorovskii, K. Golant, A. Vorotynskii, and O. G. Okhotnikov, "Optical amplifiers and lasers based on tapered fiber geometry for power and energy scaling with low signal distortion," *Proc. SPIE* **9728**, 97280V (2016).
9. V. Filippov, J. Kerttula, Y. Chamorovskii, K. Golant, and O. G. Okhotnikov, "Highly efficient 750 W tapered double-clad ytterbium fiber laser," *Opt. Express* **18**(12), 12499–12512 (2010).
10. A. I. Trikshev, A. S. Kurkov, V. B. Tsvetkov, S. A. Filatova, J. Kerttula, V. Filippov, Y. K. Chamorovskiy, and O. G. Okhotnikov, "A 160 W single-frequency laser based on an active tapered double-clad fiber amplifier," *Laser Phys. Lett.* **10**(6), 065101 (2013).
11. Z. Zhou, H. Zhang, X. Wang, Z. Pan, R. Su, B. Yang, P. Zhou, and X. Xu, "All-fiber-integrated single frequency tapered fiber amplifier with near diffraction limited output," *J. Opt.* **18**(6), 065504 (2016).

12. Z. Lou, X. Jin, H. Zhang, P. Zhou, and Z. Liu, "High Power, High-Order Random Raman Fiber Laser Based on Tapered Fiber," *IEEE Photonics J.* **9**(1), 1–6 (2017).
13. J. Kerttula, V. Filippov, Y. Chamorovskii, K. Golant, and O. G. Okhotnikov, "Actively Q-switched 1.6-mJ tapered double-clad ytterbium-doped fiber laser," *Opt. Express* **18**(18), 18543–18549 (2010).
14. X. Mu, P. Steinvurzel, P. Belden, T. Rose, W. Lotshaw, and S. Beck, "Nanosecond-pulsed, mJ-level single-mode fiber master oscillator power amplifier with polarization maintaining tapered gain fiber" in *Lasers Congress 2016 (ASSL, LSC, LAC)* (Optical Society of America, 1996), paper LW3B.2.
15. V. Roy, C. Pare, B. Labranche, P. Laperle, L. Desbiens, M. Boivin, and Y. Taillon, "Yb-doped large mode area tapered fiber with depressed cladding and dopant confinement," *Proc. SPIE* **10083**, 1008314 (2017).
16. J. Kerttula, V. Filippov, Y. Chamorovskii, K. Golant, and O. G. Okhotnikov, "250 μ J Broadband Supercontinuum Generated Using a Q-switched Tapered Fiber Laser," *IEEE Photonics Technol. Lett.* **23**(6), 380–382 (2011).
17. V. Filippov, A. Vorotynskii, T. Noronen, R. Gumenyuk, Y. K. Chamorovskii, and K. M. Golant, "Picosecond MOPA with ytterbium doped tapered double clad fiber," *Proc. SPIE* **10083**, 100831H (2017).
18. M. Yu. Koptev, E. A. Anashkina, K. K. Bobkov, M. E. Likhachev, A. E. Levchenko, S. S. Aleshkina, S. L. Semjonov, A. N. Denisov, M. M. Bubnov, D. S. Lipatov, A. Yu. Laptev, A. N. Gur'yanov, A. V. Andrianov, S. V. Muravyev, and A. V. Kim, "Fiber amplifier based on an ytterbium-doped active tapered fiber for the generation of megawatt peak power ultrashort optical pulses," *Quantum Electron.* **45**(5), 443–450 (2015).
19. V. E. Ustimchik, J. Rissanen, S. M. Popov, Y. K. Chamorovskii, and S. A. Nikitov, "Anisotropic tapered polarization-maintaining large mode area optical fibers," *Opt. Express* **25**(9), 10693–10703 (2017).
20. E. A. Savel'ev, A. V. Krivovichev, and K. M. Golant, "Clustering of Yb in silica-based glasses synthesized by SPCVD," *Opt. Mater.* **62**(1), 518–526 (2016).
21. E. A. Savel'ev, A. V. Krivovichev, V. O. Yapaskurt, and K. M. Golant, "Luminescence of Yb³⁺ ions in silica-based glasses synthesized by SPCVD," *Opt. Mater.* **64**(1), 427–435 (2017).
22. J. Kerttula, V. Filippov, Y. Chamorovskii, V. Ustimchik, K. Golant, and O. G. Okhotnikov, "Principles and Performance of Tapered Fiber Lasers: from Uniform to Flared Geometry," *Appl. Opt.* **51**(29), 7025–7038 (2012).
23. J. Noda, K. Okamoto, and Y. Sasaki, "Polarization-maintaining fibers and their applications," *J. Lightwave Technol.* **4**(8), 1071–1089 (1986).
24. J. Kerttula, V. Filippov, V. Ustimchik, Y. Chamorovskii, and O. G. Okhotnikov, "Mode evolution in long tapered fibers with high tapering ratio," *Opt. Express* **20**(23), 25461–25470 (2012).
25. "Measurement of Mode Field Diameters of Tapered Fibers and Waveguides for Low Loss Components," http://www.ophiropt.com/user_files/laser/beamprofilers/tapered_fibers.pdf.
26. M. E. Fermann, "Single-mode excitation of multimode fibers with ultrashort pulses," *Opt. Lett.* **23**(1), 52–54 (1998).
27. R. Olshansky, "Mode coupling effects in graded-index optical fibers," *Appl. Opt.* **14**(4), 935–945 (1975).
28. G. P. Agrawal, *Nonlinear Fiber Optics*, 4th ed. (Academic, Boston, 2007).
29. M. Artiglia, G. Coppa, P. Di Vita, M. Potenza, and A. Sharma, "Mode field diameter measurements in singlemode optical fibers," *J. Lightwave Technol.* **7**(8), 1139–1152 (1989).

1. Introduction

The technology of powerful fiber lasers has advanced rapidly over the last decade. High-power fiber lasers usually consist of a relatively low-power seed laser (master oscillator) and a concatenated chain of power amplifiers (so-called MOPA scheme). The main obstacles for further power scaling in fiber MOPA systems are the nonlinear effects (SBS, SRS or SPM). In order to minimize the influence of these effects and increase the output pulse energy (peak power), special active fibers with a large effective-mode area are usually used in the last stage of the amplifiers.

To date, there are several types of active fibers with a large effective-mode area (LMA) described in the literature that have been developed for high-power scaling. These are well-known LMA fibers with a low-aperture core [1], microstructured rod-type fiber [2], helical core [3] or 3C fibers [4], and tapered double-clad fibers [5]. The mode field diameter (MFD) achieved with the low aperture technologies [1–4] usually does not exceed 20–30 μ m. The microstructured rod-type fiber has a much larger MFD (up to 65 μ m [6]) and good performance. Recently, a femtosecond MOPA containing large-pitch fibers (LPF) with an impressive 2.2 mJ of pulse energy has been demonstrated [7]. The only drawback of amplification systems with LPF is their relatively long (1.2 m) unbendable rod-type fibers, resulting in a bulky and cumbersome optical scheme [7].

Previously, we have proposed an active tapered double-clad fiber (T-DCF) as a gain medium [6]. The T-DCFs have obvious advantages: a large active core diameter (up to 200 μm [8]) which allows the nonlinear effects threshold to be increased; a large area of the cladding, enabling the possibility to use low brightness; inexpensive and powerful pump sources; perfect beam quality (typically $M^2 < 1.1$); and reasonable physical dimensions (usually the coiling diameter does not exceed 35cm).

To date, many different fiber-optic lasers and amplifiers containing the T-DCF have been demonstrated: a 750W CW ytterbium fiber laser [9], high power narrowband CW amplifiers [10, 11], random tapered fiber laser [12], a nanosecond actively-Q-switched laser [13], amplifiers of nanosecond pulses [14, 15], and even a powerful pulsed supercontinuum optical source [16].

The amplification of a short pulse is one of the most promising fields for the T-DCF application. The T-DCF has already been successfully used for the amplification of nanosecond [14, 15] and picosecond pulses [5,17]. Although the advantages of the T-DCF for amplifying the pulses was first demonstrated a decade ago [5], there is still room for further improvement of their performance. In order to minimize the nonlinear effects and further increase the stored energy, it is important to use a T-DCF with the largest possible MFD, stable polarization and single-mode regime propagation of the amplified pulse. Obviously, in order to achieve stable polarization, the T-DCF must be birefringent.

To date, Yb-doped birefringent T-DCFs with a relatively modest core diameter of 45 μm [18], 56 μm [15] and 60 μm [14] have been demonstrated. Isotropic active T-DCFs with a large core diameter of 100 μm [17] and even 200 μm [8] and an anisotropic passive tapered fiber with a core size of 70 μm [19] have also been demonstrated. However, a stable and powerful pulse amplifier requires the combination of a large MFD and polarization maintenance. Therefore, there is a pressing need for a short, birefringent active T-DCF with good absorption characteristics and a large MFD supporting a strictly single-mode regime for signal amplification.

In this work, we experimentally realized and studied in detail, for the first time to the best of our knowledge, an active ytterbium-doped anisotropic T-DCF with a record-high core diameter (near 100 μm) and an effective mode area of 2000 μm^2 with an excellent output beam quality, $M^2 = 1.09$. We characterized its optical and polarization properties, and investigated the possible problems associated with a large-core tapered fiber and corresponding MFD. By implementing the anisotropic T-DCF as high power amplifier, we demonstrated experimentally the CW and pulsed picosecond MOPA with an average power of up to 70W.

2. Ultra-large core Yb-doped birefringent active tapered fiber

2.1 Geometry and absorption

The preform for our Yb-doped-silica-core fiber was fabricated using the surface plasma chemical vapor deposition (SPCVD) process. This process is free of unwanted cluster formation, has a high gain efficiency and guarantees many hours of reliable fiber operations at high optical power densities [20, 21]. The refractive index profile of the preform is shown in Fig. 1.

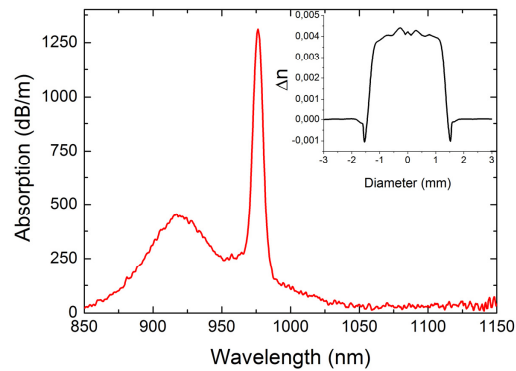


Fig. 1. In-core absorption as a function of wavelength. Inset: refractive index profile in the cross section of the preform.

The profile of the refractive index is gradient and the maximum in the center of the preform's refractive index is 0.004. The in-core small signal absorption is measured as 1270 dB/m at 976 nm (Fig. 1).

The preform for the tapered birefringent active fiber is manufactured using the stacking method. The active core part produced by the SPCVD method is surrounded by a set of different shaped and sized rods of pure and boron-doped silica, thus the fiber has panda-like structure (Fig. 2(a)). This assembly is then collapsed to a solid preform and drawn to a tapered fiber (Fig. 2b).

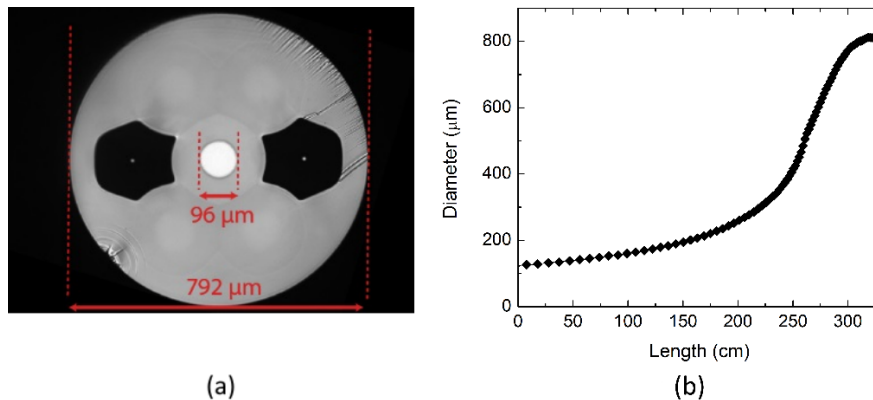


Fig. 2. (a) Cross section of active panda-type T-DCF. (b) Clad diameter versus length for T-DCF.

The core and clad diameters were 96 and 792 μm respectively (Fig. 2(a)) on the wide side of the T-DCF. The fiber tapered down to 110 μm with a tapering rate of $T = 7.2$. A typical longitudinal profile of the active taper is shown in Fig. 2(b). The total length of the tapered fiber was 360 cm. The presence of borosilicate tensile rods in the cladding leads to a good mixing of the cladding modes, and therefore no shaping of the clad is required for good clad pump absorption. The double-clad pump absorption in the T-DCF is determined by a number of parameters [22]:

- The in-core absorption at 976nm;
- The longitudinal shape of the T-DCF;
- The conditions of clad mode mixing;
- The brightness (aperture) of the pump source;

- The direction of pumping; the co-propagation and counter-propagation conditions of the pumping are different.

To avoid ambiguity, we use two main parameters to characterize the pump absorption in the T-DCF: the in-core pump absorption at 976 nm and the clad pump absorption at 976 nm for a pump propagating from the narrow end to the wide one. The first parameter is completely determined by the ytterbium concentration in the core; the second parameter is related to the ytterbium concentration in the core, the ratio between the core/clad areas, the cladding modes' mixing efficiency, the longitudinal profile of the T-DCF, and its length. The clad absorption measured in this way is independent of vignetting. The measured in-core absorption is 1270 dB/m (Fig. 1, inset) and the measured co-propagated clad pump absorption at 976 nm is 24 dB.

2.2 Birefringence measurements

The birefringence of the active T-DCF is measured by using a standard method for polarization mode beating [23]. The broadband polarized light from a 1.5 μm ASE source is launched into the narrow side of the T-DCF to excite both polarization eigenstates equally. The radiation propagated through the T-DCF is then collimated and registered by an optical spectrum analyzer.

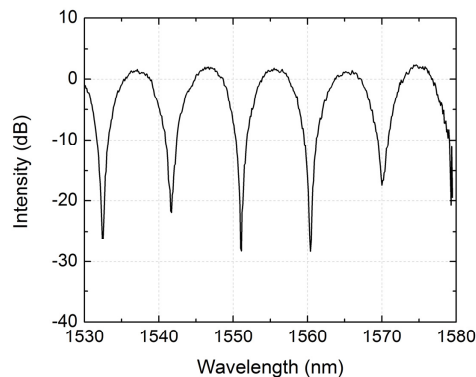


Fig. 3. Polarization mode beating in birefringent T-DCF.

The results of the measurements are shown in Fig. 3. The calculated birefringence value is 0.65×10^{-4} and the polarization extinction ratio (PER) is about 30 dB.

2.3 M^2 , divergence and mode field diameter measurements

In order to characterize the properties of an amplified beam, the M^2 and mode field diameter (MFD) are measured experimentally. The T-DCF core has a 13 μm diameter on the narrow side and a gradient index refraction profile with a maximum value of 0.004 in the center (Fig. 1). Theoretically, few modes might propagate in that waveguide at the narrow part. There are no changes in the mode content during propagation in the T-DCF, as was shown earlier in [24]. Therefore, it is extremely important to maintain a truly fundamental mode regime on the narrow side of the T-DCF. To do the selective excitation of a fundamental mode only, a $(2 + 1) \times 1$ pump combiner with a single-mode fiber at the input signal is spliced to the narrow part of the T-DCF. Measurements of the beam quality, M^2 and MFD are carried out in an amplification regime. The seed signal from a semiconductor laser diode operated at a 1035 nm wavelength with 30 mW power is launched into the narrow end of the T-DCF through an isolator and the $(2 + 1) \times 1$ multimode pump combiner. A multimode wavelength-stabilized diode (976 nm) is used as a pump source. In this experiment, the T-DCF is only pumped from the narrow side. The amplified beam has a round bell-shaped form and its parameters are analyzed with Beam Scope P7. The results of the beam quality measurements

are presented in Fig. 4. The amplifier output has an almost diffraction-limited fundamental mode with $M^2_x = 1.09$ and $M^2_y = 1.10$ respectively.

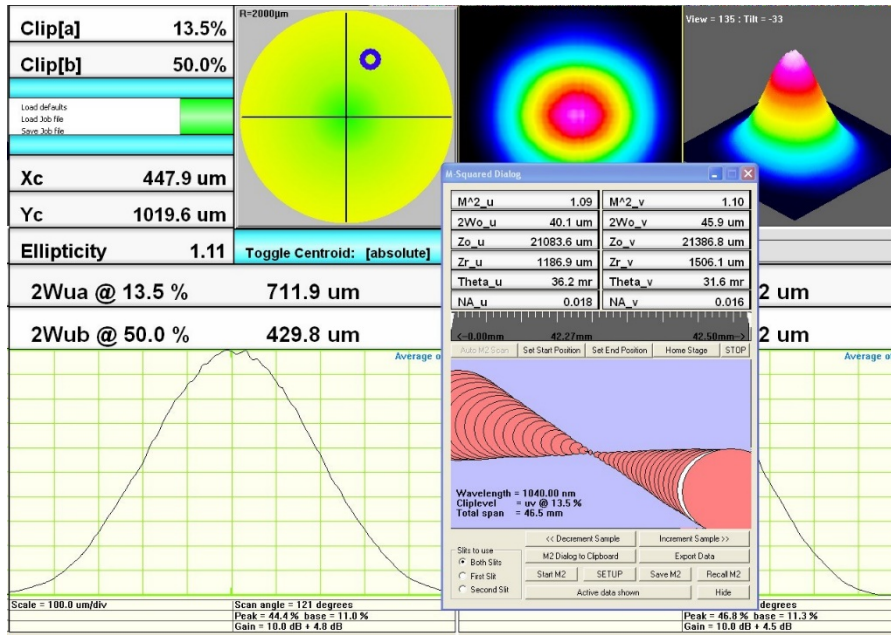


Fig. 4. M^2 measurements results.

The beam divergence is measured using an Ophir Beam star FX-66-NT beam profiler. The resulting value of the output beam is 0.026rad. We can assume that the beam profile is Gaussian due to the good M^2 value. MFD for Gaussian beams can be calculated from the formula [25]:

$$MFD = \frac{4\lambda}{\pi\theta}, \quad (1)$$

where λ is the wavelength and θ is the beam divergence. The MFD of the beam emitted by the T-DCF calculated according to (1) is 50 μ m.

2.4 The Amplification properties of T-DCF in CW mode

The amplification properties of the developed anisotropic T-DCF are investigated in the CW amplifier scheme (Fig. 5). The T-DCF is pumped bi-directionally through the fused pump combiner and dichroic mirror by fiber-coupled wavelength-stabilized diodes at 976 nm. The seed signal from the linearly-polarized CW semiconductor diode is launched into the narrow side of the T-DCF through the isolator and the fused pump combiner.

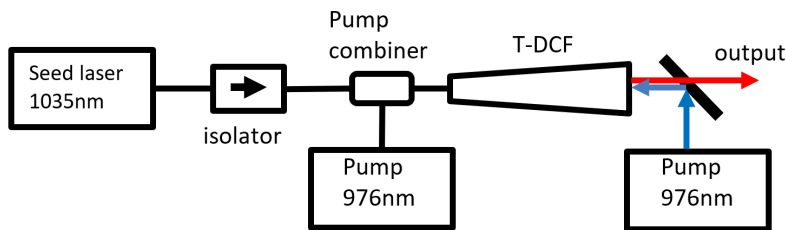


Fig. 5. The experimental set-up of CW mode amplification.

In this experiment, we investigate the dependence of the output power of the amplifier on the launched pump power (Fig. 6(a)). The maximum output power of 70 W is reached at 30 mW of input power. The total maximum pumping level is equal to 220 W. Any further increase in the input power of the seed source does not add a significant contribution to the output power, as can be seen from Fig. 6(a). The slope change in the output power versus the input power dependence is determined by switching from a uni-directional to a bi-directional pumping scheme. A small decrease in the slope is caused by vignetting effect, i.e. partial leakage of unabsorbed pump into the second cladding area. When the tapered fiber is pumped into the narrow part, vignetting is absent, and the slope efficiency is higher. When pumped into the wide side, and the absorption is not high enough some part of the pump is lost and leaks into the protective polymer. Therefore, this part of absorption is not involved in the amplification, and as a result - decrease of the slope. The dependence of the gain as a function of the input power is shown in Fig. 6(b). The amplifier has a very large gain (38 dB) and begins to demonstrate a tendency to the saturation at the input power of more than 300 mW. The spectra of the amplified CW signals for different output powers are presented in Fig. 6(c). The figure does not reveal any significant changes in the signal spectra except for the slight growth of spontaneous emission on the short-wavelength side.

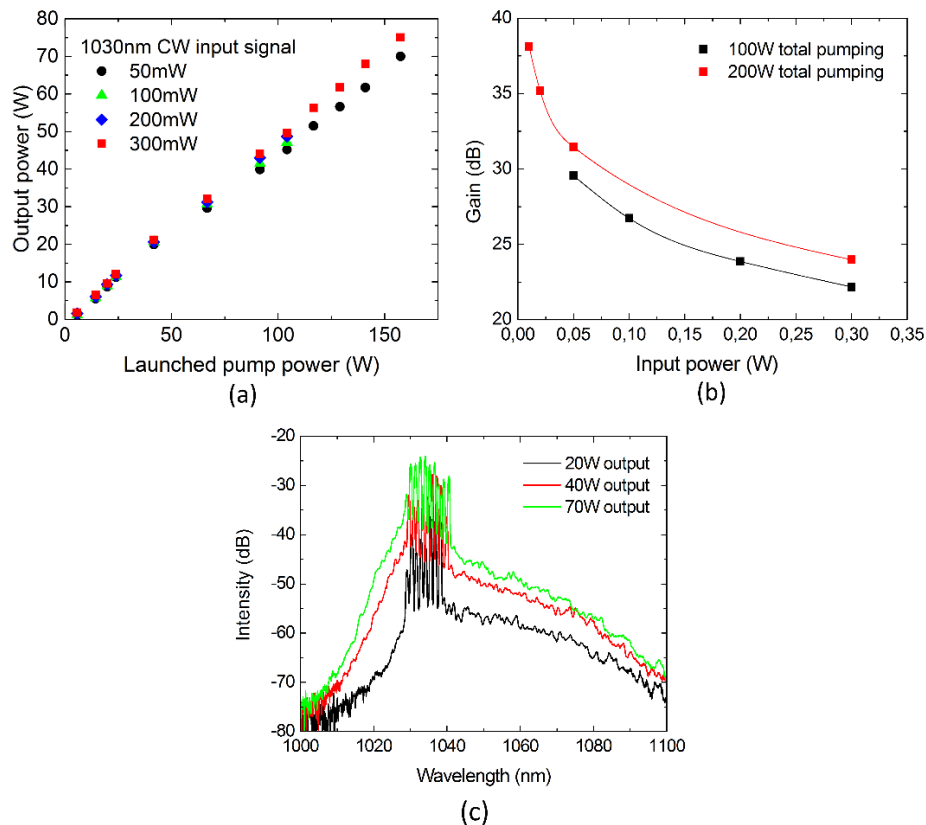


Fig. 6. CW mode amplification. (a) The output power dependence vs pump power (the slope efficiency varies from 45% for 50 mW to 48% for 300 mW), (b) gain as function of input power for 100W and 220W of the pump power, (c) spectra of amplified signal at different output power.

3. Amplification of ultrashort pulses

A buster amplifier for an all-fiber CPA system is one of the most promising fields for T-DCF application. Typically, a short optical pulse broadens to several hundred picoseconds and

then undergoes power scaling by the buster amplifier. We explore the picoseconds MOPA scheme with the T-DCF to demonstrate the potential of tapered amplifiers (Fig. 7).

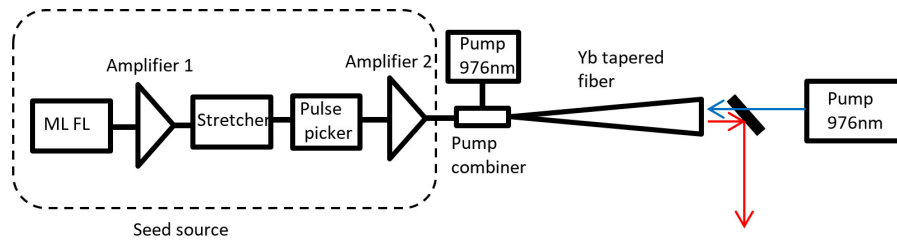


Fig. 7. Schematic of the MOPA setup for pulse amplification. ML FL – mode-locked fiber laser.

The all-fiber MOPA contains a home-made seed source (mode-locked fiber laser, MLFL), two stages of fiber amplifiers, a stretcher, a pulse picker and a high-power tapered amplifier. The all-normal dispersion fiber laser, mode-locked with a fiber-coupled SESAM, generates a pulse train with a repetition rate of 19 MHz and a 25ps pulse duration and has an average power of 1.5 mW at a 1040 nm wavelength. Both the pre-amplifiers, 1 and 2, are similar and contain 60cm Yb-doped fiber (absorption 400 dB/m at 976 nm) with a 6 μm core diameter and NA of 0.16. The amplifiers are in-core pumped by 400mW single-mode laser diodes. The first amplifier raises the output power of the mode-locked fiber laser and pre-compensates the losses in the pulse picker stage. We used 300m of Flexcore1060 fiber spool as a pulse stretcher. The pulse duration broadens to 90ps after propagation through the stretcher. The pulse picker is utilized to decrease the repetition rate from 19MHz to 1MHz. The second amplifier gains the output power to an adequate level for seeding the tapered amplifier. The maximum output power of the second amplifier is 30mW.

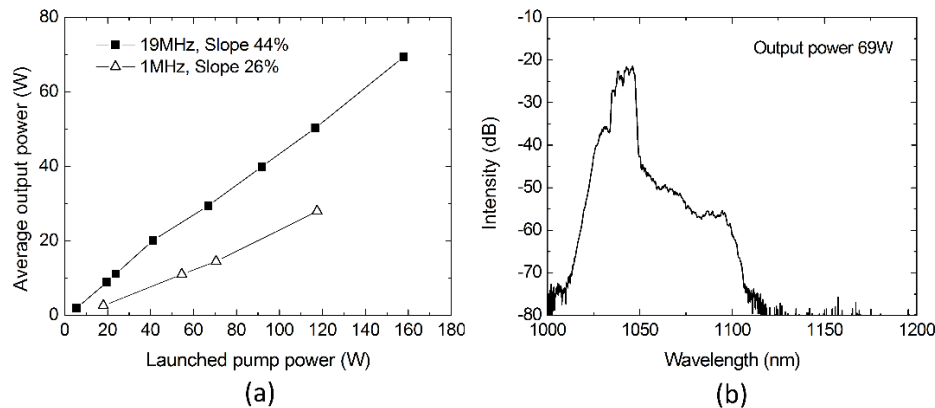


Fig. 8. Amplification of the pulse train at the fundamental frequency (19 MHz, 90ps) in a T-DCF amplifier: (a) Average output power vs launched pump power, (b) Spectrum of the output power at 69W.

This amplified emission is launched into the ytterbium-doped T-DCF pumped into the cladding from both sides (Fig. 7). The T-DCF amplifier comprises two parts (Fig. 2b): a wide and relatively short part where most of the energy is stored and most of the amplification occurs, and an arrow part which works as a pre-amplifier. Therefore, the T-DCF must be pumped from both sides. Intensively pumping the narrow side can cause significant nonlinear effects, and therefore we only launch a relatively modest proportion of the total pump power into the narrow part of the T-DCF (25W at 976nm), while the rest of it is launched into the wide side. The mode field diameter on the wide side of the T-DCF area is much larger, so we

can launch up to 160 W of pump power into the wide side. The dependence of the average output power on the launched pump power is shown in Fig. 8(a). The maximum slope efficiency is 44% for 19 MHz of fundamental repetition rate. The optical spectrum at the maximum output power is shown in Fig. 8(b). The calculated pulse energy is 3.45 μJ , which corresponds to a peak power of 36 kW.

By using a pulse picker, the repetition rate is reduced to 1 MHz, thereby increasing the pulse energy. Figure 9 shows the spectra of the amplified pulse sequences with a 1 MHz repetition rate.

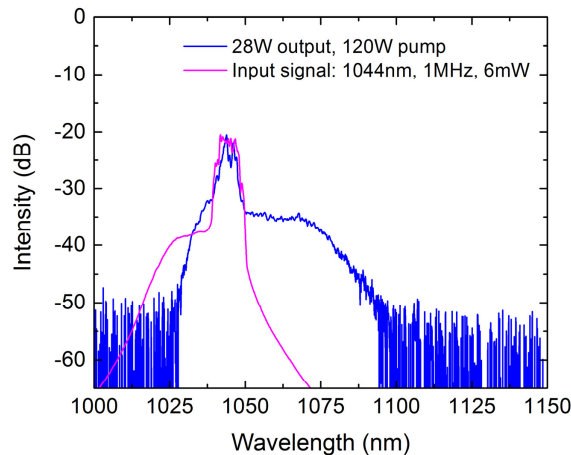


Fig. 9. Spectrum of 1MHz 90ps pulse train before and after amplification in a T-DCF.

Reducing the repetition rate leads to a rapid increase of energy and peak power, which in turn results in the Raman component's appearance. To reduce the influence of the Raman effect and enhance the shapes of the spectra, we have to decrease the amplitude of the launched seed signal down to 6 mW. As a result, the average power at the maximum available launched pump drops down to 28 W (Fig. 8(a), open triangles, slope 26%). The achieved pulse energy is 28 μJ with 292 kW of peak power. Altogether, the amplifier demonstrates a very low level of ASE, the absence of Raman components and an impressive gain of 37dB at a 1MHz repetition rate.

4. Discussion

Currently, there are several types of active amplifying fibers with a large mode-field diameter, in which different approaches (strategies) are used to achieve the propagation of a single mode with a large mode-field diameter. For example, for LMA fibers, the strategy is to create different losses for the fundamental and higher-order modes when bending a fiber with a small core aperture. In 3C fibers, the effect of wave propagation in coupled waveguides is used with the subsequent dissipation of the higher-order modes in the cladding. In microstructured fibers, a sufficiently small difference in the refractive indices of the core and cladding is realized in order to support the propagation of only a single mode.

In active tapered fibers, the strategy of realizing the propagation of only one mode consists in the initial selective excitation of only a single fundamental mode in the narrow side of the tapered fiber, and then maintaining the propagation of only one mode in the wide multimode side T-DCF. As it was shown experimentally by Fermann [26] if in a multimode fiber with a thick cladding to excite only one mode, then it will propagate over tens of meters without changing the mode composition. The reason for this effect is the fact that the mode coupling coefficient in multimode fibers strongly depends on the outer diameter of the fiber (inversely proportional to the diameter of the cladding in the 6th degree) [26, 27]. Since in our case the coefficient of the tapering is 7, the coefficient of mode coupling in the wide part

of the taper is 7^6 times smaller than the modal coupling coefficient in its narrow part. The taper is slightly bent (spooled with a diameter of 35 cm), and, therefore, the effect of mode coupling, which can potentially lead to a change in the mode composition and as a result to the degradation of M^2 , is negligible. This is effect can be preserved by avoiding local perturbations in the multimode part of the T-DCF, i.e. splices, small-radius bends, etc.

Moreover, in the single-mode part of a tapered fiber, the effective MFD may be greater than the core diameter, and as the core diameter increases, the effective MFD also increases to reach a constant value for the ratio with the core diameter. The variation of the mode-field diameter along the tapered fiber length can be calculated from the definition of the effective mode area given in Refs. 28, 29

$$A_{eff} = \frac{\left[\int_{-\infty}^{\infty} \int_{-\infty}^{\infty} |E(x, y)|^2 dx dy \right]^2}{\int_{-\infty}^{\infty} \int_{-\infty}^{\infty} |E(x, y)|^4 dx dy}, \quad (2)$$

where $E(x, y)$ is the optical field distribution. The size of the effective MFD in a step-index fiber depends on the diameter of the core and is determined by the formula

$$d_{eff} = \frac{2\sqrt{2} \int E_i^2 r dr}{\left[\int E_i^4 r dr \right]^{1/2}}, \quad d_{eff} = \frac{2}{\sqrt{\pi}} \sqrt{A_{eff}} \quad (3)$$

Figure 10 shows the dependence of the MFD on the core diameter calculated in accordance with (3) for numerical apertures 0.1 (value for the active taper) and 0.06, 0.16, 0.22 (for comparison).

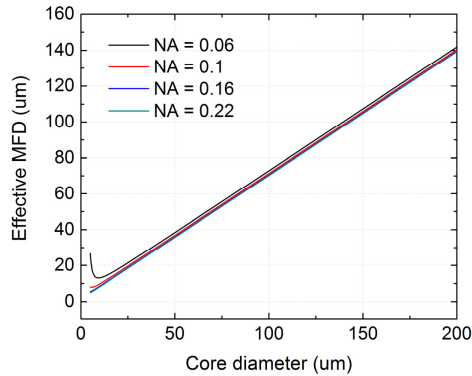


Fig. 10. Effective mode field diameter as a function of core diameter for core NA 0.1 (red line), 0.06 (black), 0.16 (blue), 0.22 (green).

As follows from formula (3) and the results shown in Fig. 10, the size of the MFD is linearly dependent on the core diameter of the step-index fiber with aperture 0.1, and it can be approximated by the following linear dependence:

$$MFD = 2.39 + 0.69D[\mu\text{m}] \quad (4)$$

The dependence of the effective MFD on the core diameter is linear and almost independent of the numerical aperture of the core for large diameters (Fig. 10). Since the core diameter varies with the length of the active tapered fiber, formula (4) explains the large size of the mode spot in the wide part of the active T-DCF. It follows from (4) that, theoretically, for a taper with a stepped profile of the refractive index, the effective MFD size is approximately 70% of the core diameter. However, this is true only for an ideal profile of the

refractive index, which is rarely achieved in real conditions. In a real preform, there is always some modulation of the refractive index profile in the cross section, which leads to distortion of the shape of the output beam. Experimentally, in [24] it was shown that for long passive tapered fibers that have an ideal refractive index profile, the presence of mechanical stresses in the core eventually leads to the fact that only the LP_{01} mode remains, which takes the form of a ring. In our case, the profile of the refractive index also has a small modulation (within $\pm 5 \times 10^{-4}$), which eventually leads to a certain decrease in the size of the mode-field diameter to $50 \mu\text{m}$, compared with the expected theoretical limit of $69 \mu\text{m}$. The beam shape remains Gaussian and the beam quality (M^2) is high.

The ability to preserve polarization is another important property of an active anisotropic tapered fiber. Recently, the evolution of birefringence over the length of an anisotropic tapered fiber with a pre-stressed cladding and a core diameter of up to $70 \mu\text{m}$ was studied [19]. One of the important results of this study is the conclusion that, although birefringence in a tapered fiber varies with length, the changes are insignificant; less than 10% at a tapering ratio of 7-10. Thus, despite some reduction in birefringence with length, a tapered fiber remains birefringent and, as a result, maintains polarization. Another important conclusion of the paper [19] concerns the small coupling of the polarization modes in a tapered fiber with a large tapering ratio.

The results of our measurements of mode beat for active T-DCF are in good agreement with the results of Ref. 19. Although the polarization beat length is not very high, 16mm (0.65×10^{-4}), the polarization extinction in the 4th piece of fiber wound with a diameter of 35cm was 30dB (Fig. 3). The maintenance of such a high polarization is due to a combination of such factors as the short length of the tapered fiber, a significant intrinsic birefringence and the absence of any significant perturbations (diameter of winding 35 cm or even less).

5. Conclusion

We demonstrated a compact and robust amplifier based on active birefringent tapered double-clad fiber operating in a strictly single-mode regime with an ultra-large core diameter equal to $96 \mu\text{m}$ and excellent beam quality ($M^2 = 1.09$). The tapered fiber amplifier was characterized by its high polarization/extinction ratio, which reached 30 dB . The active birefringent tapered double-clad fiber was explored for high power amplification of the signal from a linearly-polarized CW laser diode and a mode-locked fiber laser. An average output power of 70 W was achieved for the CW regime. In the case of 90 ps pulses at a 1MHz repetition rate, the T-DCF provides an amplification up to the level of 28 W with a 37 dB gain and a pulse energy of $28 \mu\text{J}$. At that point the spectrum was free of Raman components. Since the pulses were initially stretched to 90 ps before the amplification, there is a great potential to achieve record peak power through further pulse compression.

We derived a linear dependence of the MFD with the core diameter for tapered double-clad fiber characterized by single-mode operation and a numerical aperture of 0.1. The maximum MFD that can be reached is composed of approximately 70% of the core diameter. Therefore, for a tapered fiber with a $96 \mu\text{m}$ core diameter, the maximum MFD would not exceed $69 \mu\text{m}$. The MFD of the tapered fiber described in this article obtained as much as $50 \mu\text{m}$, corresponding to an effective mode area of almost $2000 \mu\text{m}^2$. The reduction of the MFD value was due to the strong effect of the small modulation in the refractive index of the core. In order to achieve a single-mode regime in the active tapered fibers, it is necessary to minimize the fiber's inhomogeneities, e.g. the refractive index profile, splices and small radius bends etc. This is particularly crucial for the highly-multimode tapered fiber part. If there is even a small perturbation and a large core size ($100 \mu\text{m}$), this can lead to distortion of the fundamental mode shape, which deviates from the Gaussian shape, and also leads to a change in the fundamental mode-size.

Funding

Ministry of Education and Science of the Russian Federation (grants No. 16.3788.2017/4.6 and 16.4959.2017/6.7); Academy of Finland (Project No. 285170); Russian Foundation for Basic Research (RFBR) (16-37-60010 mol_a_dk).